batteries

Article

Experimental Research on the Ignition Characteristics and Inhibition Strategy for Venting Emissions Mixture of Failure $LiFePO_4$ Battery

Yan Wang [1,*], Zhaozhi Zhang [1], Ruiguang Yu [1], Yalun Li [2], Hewu Wang [2], Languang Lu [2], Xuning Feng [2] and Minggao Ouyang [2]

[1] School of Mechanical and Automotive Engineering, Qingdao University of Technology, Qingdao 266520, China; zhangzhaozhi@stu.qut.edu.cn (Z.Z.); ruiguang.yu@bjtu.edu.cn (R.Y.)
[2] State Key Laboratory of Automotive Safety and Energy, Tsinghua University, Beijing 100084, China; lyl17@mails.tsinghua.edu.cn (Y.L.); wanghw@tsinghua.edu.cn (H.W.); lulg@tsinghua.edu.cn (L.L.); fxn17@mail.tsinghua.edu.cn (X.F.); ouymg@tsinghua.edu.cn (M.O.)
* Correspondence: wang_yan@qut.edu.cn

Abstract: When the concentration of a gas is below its lower flammable limit and the content of a liquid is below its minimum explosible concentration, their combined fuel mixture can be ignitable. The flammability characteristics and inhibition strategies for battery emission mixtures deserve further in-depth research attention. This article presents experimental research on the ignition characteristics and inhibition strategy for a venting emission mixture of a failure $LiFePO_4$ battery. By identifying the components of venting emissions, ignition experiments for gases, electrolyte mist, their combination fuels, and mixtures with additives are performed to determine the flammable parameters, including ignition sensitivity and severity. The hybrid combination of non-flammable venting gases and electrolyte mist has the potential to induce ignition. However, there still exists a non-ignition region, where the gas concentration ratio (m_g) is below 0.15 and the liquid concentration ratio (m_l) is below 0.1. A safety design principle can be proposed: increasing ignition temperature, prolonging ignition time, and reducing maximum pressure. Adhering to this principle, a non-flammable electrolyte consisting of 1 mol $LiPF_6$ in EC:DEC = 1:1 vol%, with FEC at 10% and VC at 1%, can be considered as an optimization strategy. In comparison to the original gas–liquid mixtures, the region where no ignition occurs becomes wider when both the m_g is below 0.45 and the m_l is below 0.3. The new two-phase mixture has an ignition temperature of 835 °C, which is, respectively, 50% higher than that of the original mixture. Overall, this experimental research demonstrates an innovative methodology for assessing the battery venting emission mixture safety while proposing a design principle for modifying non-flammable electrolyte functional materials. Consequently, these findings can contribute to formulating more suitable preventive and protective measures for commercial electric vehicles and battery energy storage systems' thermal safety designs.

Keywords: lower flammable limit; venting emission; ignition sensitivity; ignition temperature

Citation: Wang, Y.; Zhang, Z.; Yu, R.; Li, Y.; Wang, H.; Lu, L.; Feng, X.; Ouyang, M. Experimental Research on the Ignition Characteristics and Inhibition Strategy for Venting Emissions Mixture of Failure $LiFePO_4$ Battery. *Batteries* **2024**, *10*, 423. https://doi.org/10.3390/batteries10120423

Academic Editor: Marco Giorgetti

Received: 21 October 2024
Revised: 19 November 2024
Accepted: 26 November 2024
Published: 30 November 2024

1. Introduction

The urgent imperative to address the global energy crisis and environmental pollution has resulted in the significant and thriving development of electrification in transportation and energy storage [1]. At present, the research progress of new battery systems is rapid; for example, $(Ni_9Co_{0.5}Mn_{0.5})\ O_2$ $(Ni_8Co_1Mn_1)\ O_2$ and other systems are also emerging [2]. However, LFP LIBs have been extensively embraced in the realm of electrical vehicles (EVs) and battery energy storage systems (BESS) [3].

However, due to the abundance of active materials and electrochemical energy within LIBs' cathode, anode, and electrolyte components, they are susceptible to thermal runaway (TR), particularly when subjected to unexpected abusive conditions [4]. It is undeniable

that safety concerns arising from internal electrochemical reactions have posed a bottleneck for LIB development [5].

Among the component of LIBs, organic electrolyte solvents used in these batteries are flammable chemicals such as ethylene carbonate (EC), ethyl methyl carbonate (EMC), dimethyl carbonate (DMC), and diethyl carbonate (DEC). Due to the throttling effect of the safety valve, the liquid electrolyte evaporates and absorbs heat generation for TR. Additionally, during this venting flow (VF) process, battery venting gases (BVGs) and electrode particle dust are commonly mixed with electrolyte liquid [6,7]. Consequently, the hybrid mixture jet flow during TR is a hot and difficult topic in the field of LIB TR, risk assessment, and fire prevention [8].

The gas components in both NCM and LFP batteries mainly include H_2, CO, CO_2, C_2H_4, and CH_4. LFPs have a higher proportion of H_2. Peng et al. [9] identified the major toxic gases in a 68 Ah LFP through online analysis. The major gases detected were CO, HF, SO_2, NO_2, NO, and HCl. As for the identification of VF particle components, the author's team [10] used scanning electron microscopy and energy-dispersive X-ray spectroscopy (SEM-EDS) to analyze and assess elements in smoke particles from an abused prismatic NCM_{622} battery. Regarding battery electrolyte venting, Wang employed high-speed photography to capture the rapid VF for LIBs in an N_2 atmosphere. Their results captured images showing characteristics of gas–liquid–solid three-phase coexistence [11].

As for LIB VF, gases, electrolyte liquids, and electrode particles have different combustion and explosion characteristics, and the ignition mechanism of hybrid mixture flammability needs to be studied synergistically [3,4,8]. It was shown that it can become explosive when the gas concentration is below its lower combustible limit and the particle content is below its minimum combustible concentration. Furthermore, both particle size and gas content significantly impact the flammability characteristics of this hybrid mixture. NCM battery venting can release hot solid particles that ignite the flammable gases, while LFP LIBs' VF typically consists of electrolyte mist and gases [8]. There is still a research gap in determining the ignition conditions for emission mixtures combined with gas–liquid, particularly in terms of sensitivity and severity for LFP LIBs.

The above comprehensive research can be used to build a database for TR in LIB incidents, which can significantly improve the TR forewarning and prevention measures [3]. The TR emergency strategy and prevention method mainly includes water mist, liquid nitrogen, etc. [12,13]. Additionally, flame-retardant additives for electrolytes have been extensively proven to enhance battery thermal safety performance [14]. Tim Dagger presented that FPPN can serve as a stable electrolyte additive, simultaneously improving intrinsic safety and cycling performance [15]. Hu et al. [16] discovered that adding 10 vol.% DEMEMPA to a 0.9 M LiPF6/EC/DMC solution can effectively suppress electrolyte combustion and widen the electrochemical window. Bahareh Dadeghi reported the optimal concentration of PhEPi along with two well-known film-forming additives, namely vinylene carbonate (VC) and fluoroethylene carbonate (FEC), which exhibited the complementary advantages of high specific discharge capacity and prolonged cycle life [17].

These typical chemicals include borate, phosphate, nitrate, and phosphite compounds, as well as polymers and additional additives. The addition of flame retardants can effectively suppress the formation of solid electrolyte interphase and dendrite layers, enhance thermal stability, extend lifespan, and improve cycling characteristics [18]. However, there is still a lack of systematic understanding regarding the impact of these additives on inhibiting flammability in battery venting emissions.

The aim of this paper is to investigate the following questions: What are the flammability properties of the LFP electrolyte and its two-phase mixture? What is the inhibitory effect on flammability for VF emissions by non-flammable additives?

To address the research gap in understanding the ignition sensitivity and severity parameters of hybrid mixtures of battery vent gas and electrolyte mist, an experimental study of a 120 Ah LFP LIBs in an inert atmosphere is presented in this paper. Experiments are carried out on venting gases, electrolyte mists, their combined mixture fuels, and a

mixture fuel with different additives. The aim of this work is to provide a comprehensive understanding of the LIB venting emissions, for both single-phase and gas–liquid two-phase mixtures. The findings from this paper significantly contribute to the future rational design of functional materials and the development of more suitable preventive measures for thermal safety design in commercial LIBs.

2. Experimental Methodology

2.1. Methodology Framework

To investigate the ignition sensitivity parameter and severity parameter for thermal failure battery emission, the below framework (Figure 1) is adopted in this article. The key to distinguishing failed LIBs' emission flammability is the identification of its components. Thus, firstly, the LIBs' thermal runaway experiment is conducted. With a gas-collection bag, the gas components and proportion can be determined by GC. According to the remaining liquid, the battery electrolyte formulation can be deduced. With a clear sense of the emission component, the gas cylinders and electrolyte can be prepared to implement the flammability parameters for the gases/electrolyte and their mixture. According to the flammability test, a 20 L sphere apparatus is adopted. Furthermore, the flammability inhibition effect for the gas–liquid mixture with additives shall be discussed.

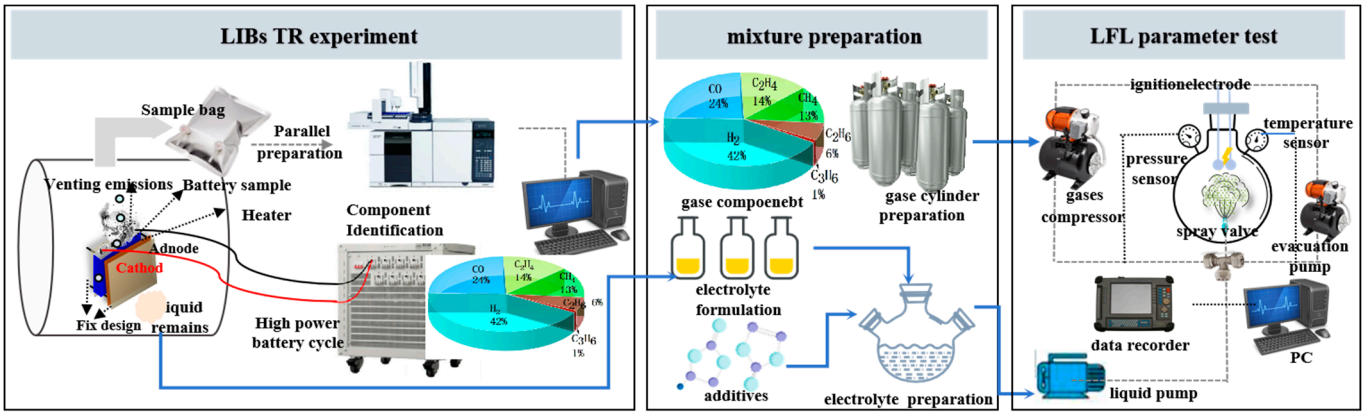

Figure 1. Test framework.

2.2. Thermal Runaway Experimental

2.2.1. Thermal Failure Test

(1) Sample battery

The TR experiment employed 120 Ah LIBs, which can be selected for BESS applications. The positive electrode material was $LiFePO_4$, while the negative electrode material was graphite. It possessed a rated capacity of 120 Ah and dimensions measuring 174 × 170 × 48 mm. The initial weight amounted to 2868 g, and it operated at a rated voltage of 3.2 V. The electrolyte formula was 1 mol LiPF6 in EC:DEC = 1:1 vol%.

(2) Thermal failure trigger

As shown in Figure 1, the LFP thermal failure test was conducted in the experimental chamber with an N_2 atmosphere, which was utilized in a previous study in Reference [8]. The chamber had a volume of 1000 L capable of withstanding the maximum pressure of 5 MPa. The heater power was 1000 W. The battery and heater were fixed closely with the assembly parts, with the preload set to 2000 N·m.

2.2.2. Component Identification

(1) Mass loss

The mass is recorded before and after the TR tests. As shown in Figure 2, before the tests, the LFP cell's initial mass is 2868 g. The mass for the remaining LFP is 2262 g after TR.

And it should be noted that there is residual liquid below. This liquid can be collected and weighed to be 90 g.

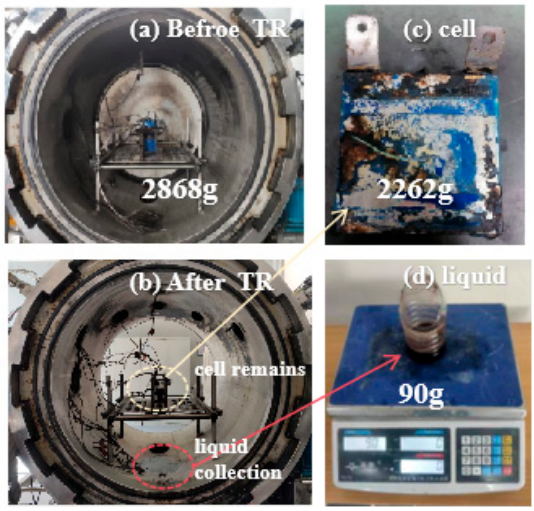

Figure 2. LIBs TR: (**a**) Before test. (**b**) After the test, (**c**) the cell retains its mass. (**d**) Liquid-collection mass.

(2) Gas component

For the test, we prepared an LFP cell and two sample gas bags. After the TR tests ended, the sample gas bags could be used to collect the internal emissions for competent identification. Parallel sampling was conducted with GC-MS, and the battery component distribution could be determined. The results of the two parallel tests for gas component proportions are shown in Figure 3.

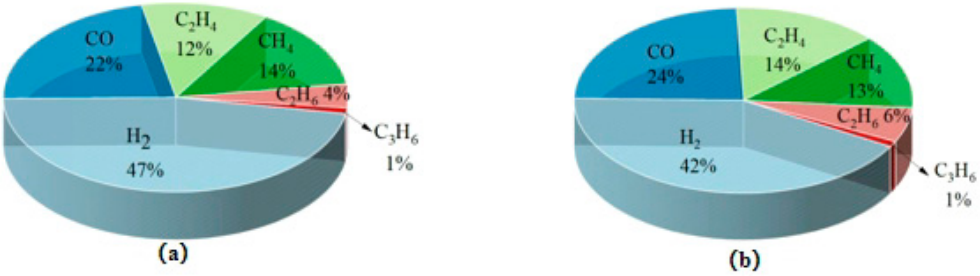

Figure 3. Gas component: (**a**) The first test's results; (**b**) The second test's results.

As shown in Figure 3a, the proportions of CH_4, C_2H_6, C_2H_4, C_3H_6, CO, and H_2 are 14%, 4%, 12%, 1%, 22%, and 47%, respectively. As shown in Figure 3b, the proportions of CH_4, C_2H_6, C_2H_4, C_3H_6, CO, and H_2 are 13%, 6%, 14%, 1%, 24%, and 42%, respectively. Among them, H_2 has the highest proportion, followed by CO, with a relative error of <5%. The relative concentration error for CO is 4.5%, and for H_2, it is 11.9%. This indicates that the test results have good repeatability. Additionally, the flammability tests follow the gas component results in Figure 3a to prepare the gases.

2.3. Flammability Test

2.3.1. Ignition Experimental

(1) Ignition apparatus

The flammability tests were conducted in a 20 L sphere apparatus to determine the ignition characteristics. A diagram of the 20 L sphere apparatus is shown in Figure 1. The experimental apparatus consists of a sphere with an internal volume of 20 L, ignition spark electrodes, a vacuum pump for the evacuation of the chamber, temperature/pressure sensors, a data recording system, an electrolyte vessel and gas cylinder, and a spray valve

for the distribution of the electrolyte. The mentioned parts are in accordance with the previous study [8]. The bottle is a 0.2 L chamber, and the fuel injection nozzle is modified for liquid ejection. The ignition electrode is placed at the center of the sphere through a flange located at the top of the combustion chamber. The standardized ignition source is an electrically generated spark igniter capable of delivering an ignition energy of up to 10 J according to international standards (EN 14034-1-4) [19].

(2) Flammability parameter

The flammability tests can be performed for individual components or mixtures, which consist mainly of gas, spray mist, and their combination. The results are called ignition characteristics; for example, the ignition temperature (IT), ignition time, lower flammability limit (LFL) for gases, and minimum explosive concentration (MEC) for electrolyte are named ignition sensitivity parameters, which represent the degree of difficulty to ignite the fuel. A lower ignition temperature, a short ignition time, and a lower LEL/MEC usually mean that the fuel ignites easily.

Accordingly, the ignition severity can be estimated by the intensity parameters, including maximum explosion pressure (P_{max}), maximum rate of pressure rise $(dP/dt)_{max}$, and pressure propagation rate coefficient (PC). Usually, a larger value of P_{max} indicates a more severe destructive effect. A lower value of $(dP/dt)_{max}$ and PC indicates that the pressure propagation rate is faster and the gradient is larger. Based on the above parameters, LIBs' single- or multiple-phase emission components' ignition likelihood and explosion severity can be understood in depth.

2.3.2. Ignition Test Procedure

(1) Venting gases

This 20 L spherical chamber was initially filled with air at atmospheric conditions. To provide the correct content for gas volume concentration in the ignition experiments, the partial pressure method was used. Therefore, the pressure sensor could precisely measure the internal pressure gauge. The pressure, then, was evacuated to be 0.3 bar. An automatic test sequence was initiated to pressurize the fuel, and then a fast-acting spray valve was used to inject the fuel into the sphere chamber through a rebound nozzle. The rebound nozzle ensured an even distribution of fuel within the sphere chamber. After being filled with the air/combustible gas mixture, the sphere vessel was stirred continuously until satisfactory homogenization was achieved by mixing the system and stirring the vessel for 5 min. The ignition spark control system activated the spark electrodes to ignite the gaseous fuel at the center when the fuel was homogeneously dispersed.

(2) Electrolyte mist

To investigate the explosion characteristics of liquid sprays, a similar principle to the gas test was applied. Firstly, a defined amount of electrolyte was introduced into the liquid bottle with a pipette. After the introduction of battery electrolyte into the liquid bottle, the bottle was then filled with compressed air. Then, the ignition apparatus sphere was evacuated to a pressure below the vapor pressure of the respective electrolyte. Upon opening the valve, the liquid bottle was connected to the rebound nozzle in the 20 L ignition apparatus. The liquid sprayed as a fine mist into the 20 L sphere. The average Sauter mean diameter of the liquid mist droplets based on the specification of the nozzles can be within the range of 7 to 17 μm.

(3) Mixture fuel

The two-phase hybrid mixture fuel can be a liquid mist of gas and electrolyte. The ignition testing procedures for a hybrid mixture are meant to introduce the material in another solvent in the 20 L sphere chamber. Considering the gas–electrolyte liquid mist as the analytical subject, the gas and electrolyte can be injected into the 20 L chamber after the sphere has been evacuated. There are two points that should be noted for the hybrid mixture ignition experiments. Firstly, it has been shown that hybrid mixtures can also be

explosible when both the concentrations of the liquid and the gas are below their respective explosible limits. When preparing the hybrid mixture, the gas volume concentration and liquid mist mass concentration should both be below the LFL. Additionally, when gas can be added to the ignition sphere after evacuation, the pressure should be less than 0.4 bar to leave space for the gas and liquid.

3. Ignition Parameter Characteristics

3.1. Mixture Preparation

(1) Gases

According to the testing method in Section 2.3.2, the ignition parameters for battery venting gas are listed in Table 1. It can be seen that the volume concentration is 4.5% for LFL.

Table 1. Venting gases ignition parameters.

Venting Gas Mixture	Sensitivity Parameters			Severity Parameters		
	Concentration (vol %)	IT (°C)	Ignition Time (ms)	P_{max} (kPa)	$(dP/dt)_{max}$ (MPa/s)	P_C
LFL	4.52	435	10	450	34.9	9.48

(2) Electrolyte

According to the above testing method in Section 2.3.2, the ignition parameters for battery electrolyte liquid with the formula of 1 mol $LiPF_6$ in EC:DEC = 1:1 vol% can be determined in Table 2.

Table 2. Electrolyte liquid ignition parameters.

Venting Electrolyte	Sensitivity Parameters			Severity Parameters		
	Concentration (g/m^3)	IT (°C)	Ignition Time (ms)	P_{max} (kPa)	$(dP/dt)_{max}$ (MPa/s)	P_C
LFL	165.5	535	10	550	44.9	12.20

(3) Mixture fuel preparation

As is known, when the concentration of gas is below its LFL and the content of the electrolyte is below its MEC, it can be explosible. According to the experimental procedures in Section 2.3.2, the gas and electrolyte concentration should be below their LFL/MEC. As for the battery venting gas with an LFL of 4.5%, the gas volume concentration in the admixture should be lower than 4.5%. As for the battery liquid electrolyte with an LFL of 165.5 g/m^3, the liquid mist mass concentration in the admixture should be lower than 165.5 g/m^3.

To determine the ignition conditions for emissions mixtures ignition, the preparation for the non-explosive gas and electrolyte liquid is shown in Table 3.

$$m_g = \frac{\text{volume}}{LFL_g} \quad (1)$$

$$m_l = \frac{\text{mass}}{MEC_l} \quad (2)$$

Table 3. Two-phase mixture preparation for the ignition test.

Gas		Electrolyte	
Concentration (vol%)	**m_g**	**Concentration (g/m^3)**	**m_l**
1	11%	11	7%
2	22%	22.5	14%
3	44%	45	27%
3.5	78%	90	54%
4	90%	135.5	82%

3.2. Sensitivity Parameters

The IT and ignition time for the gas–electrolyte (1 mol $LiPF_6$ in EC:DEC = 1:1 vol%) mixtures can be seen in Figure 4. These two index parameters denote the difficulty degree/likelihood of mixture ignition. Higher values of IT and ignition time suggest a lower likelihood of ignition, with lighter colors indicating a safer condition and red color indicating a hazard. It can be found that the non-flammable region has a 10 J sparkle electrode, where $m_g < 0.15$ and $m_l < 0.1$.

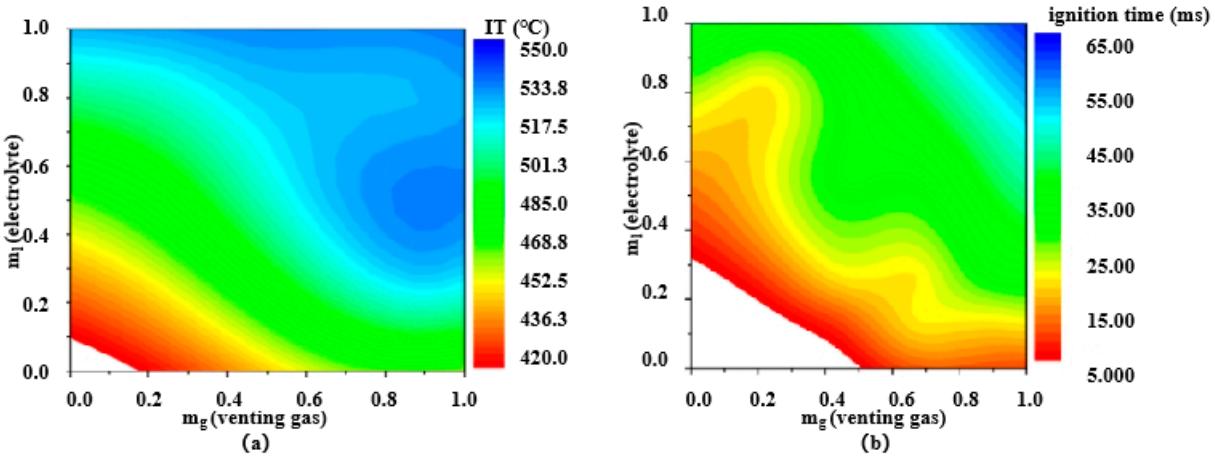

Figure 4. Ignition parameters for the gas–electrolyte mixture: (**a**) IT, (**b**) ignition time.

3.2.1. Effect of Liquid Concentration

As shown in Figure 4a, the IT increases with an increase in electrolyte liquid concentration (m_l) while keeping the gas content (m_g) stable. For instance, when $m_g = 0.5$ and the gas–liquid concentration ratio pair (m_g, m_l) is (0.5, 0.2), the IT is 470 °C. As m_l increased to 0.8, and the (m_g, m_l) became (0.5, 0.8), the IT reached 528 °C, which represents a growth of 10.2%.

As demonstrated in Figure 4b, while maintaining a stable gas content, an increase in the electrolyte liquid mist concentration leads to a delay in ignition time. For example, when $m_g = 0.5$ and (m_g, m_l) is (0.5, 0.2), the ignition time is 5 ms; however, as the liquid concentrations rise to reach (m_g, m_l) values of (0.5, 0.8), the ignition time is 18 ms, representing an increase by a factor of 2.6.

3.2.2. Effect of Gas Concentration

When m_l is kept stable, the IT increases with the increase in gas concentration. For example, when $m_l = 0.5$, the (m_g, m_l) is (0.2, 0.5), and the IT is 462 °C; when m_g increased to 0.8, the (m_g, m_l) is (0.8, 0.5), and the IT is 542 °C, which can be increased by 17.2%.

As shown in Figure 4b, when m_l is kept stable, the ignition time increases with the increase in m_g. For example, when $m_l = 0.5$, the mixture concentration ratio pair (m_g, m_l) is (0.2, 0.5), and the ignition time is 10 ms. As m_g increased to 0.8, the mixture concentration

ratio pair (m_g, m_l) is (0.8, 0.5), and ignition time increased to 32 ms, which can be multiplied by 2.2 times.

3.2.3. Influential Analysis

As m_g or m_l gets larger, IT increases. As IT is higher, the harder it is for combustion to be triggered, where blue is used to represent the ignition unlikelihood. However, as m_g gets larger, or as m_l gets larger, the ignition time increases. It can be inferred that as ignition time increases, the harder it is for the combustion to be triggered, where blue is used to represent the ignition with a smaller possibility. A conclusion that can be drawn is that when either mg or ml is constant and the other parameter is increasing, the IT and ignition time get larger, indicating the increase in ignition unlikelihood.

3.3. Severity Parameters

The index parameters of P_{max}, $(dP/dt)_{max}$, and P_c represent the mixture combustion energy and its release rate. A large P_{max} usually denotes that a massive impact will be caused. A high $(dP/dt)_{max}$ and P_c typically indicate an increase in combustion turbulence kinetic energy, leading to the generation of blast shock and vibration. The three index parameters reflect ignition severity. The venting gases' and electrolyte–liquid mixture's ignition severity parameters can be seen in Figure 5, which also indicates the non-ignition region with the mixture concentration ratio pair (m_g, m_l) below (0.15, 0.1).

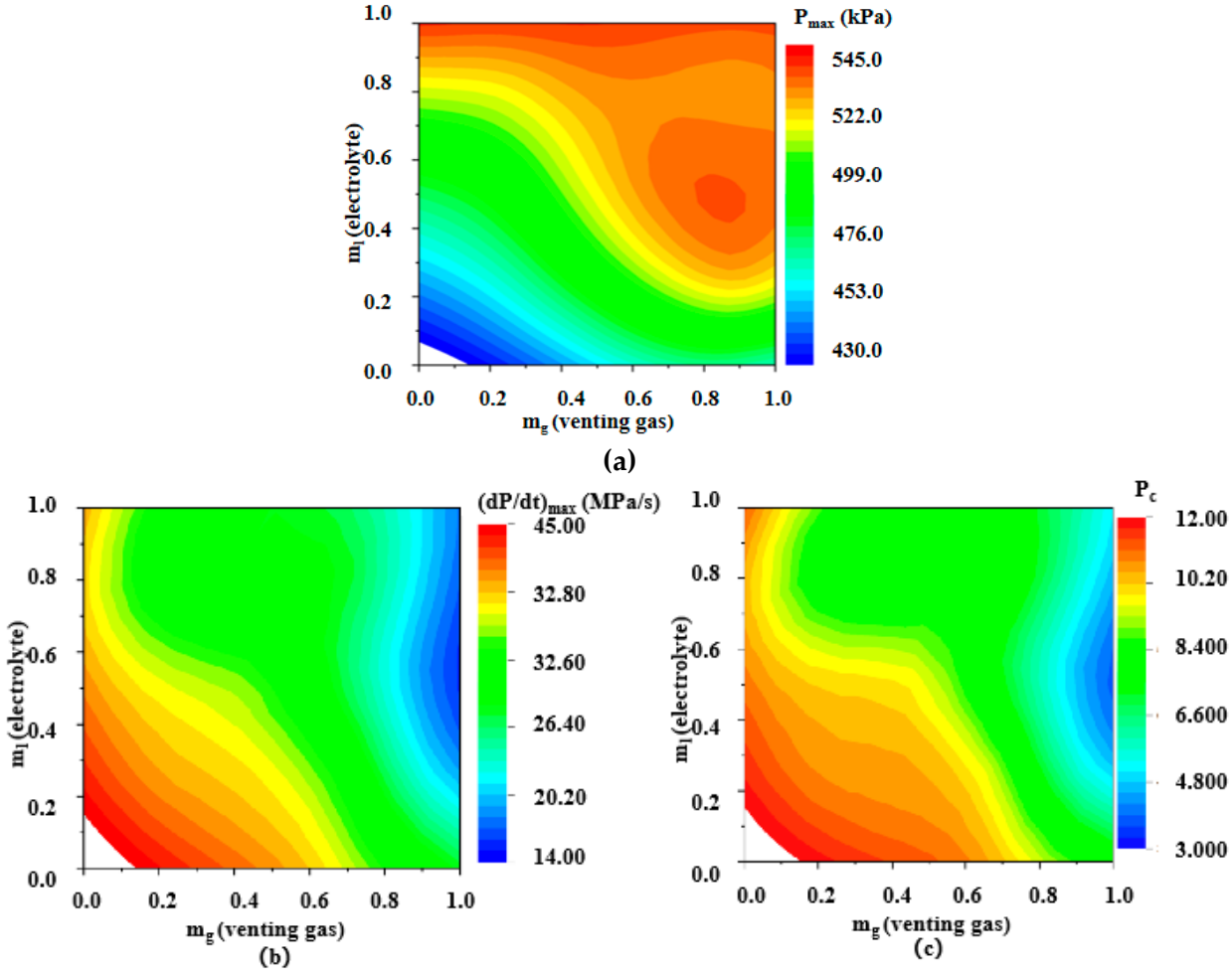

Figure 5. Ignition severity for mixture (**a**) P_{max}, (**b**) $(dP/dt)_{max}$, and (**c**) Pc.

3.3.1. Liquid Concentration Effect

As shown in Figure 5a, when the m_g is kept stable, the P_{max} increases with an increase in m_l. For example, when m_g = 0.5, the mixture concentration ratio pair (m_g, m_l) is (0.5, 0.2), and the P_{max} is 476 kPa. As m_l increased to 0.8, the mixture concentration ratio pair (m_g, m_l) is (0.5, 0.8), and the P_{max} is 520 kPa, which can be increased by 10.2%.

As shown in Figure 5b, when m_g is stable, the $(dp/dt)_{max}$ decreases with an increase in m_l. For example, when m_g = 0.5, the mixture concentration ratio pair (m_g, m_l) is (0.5, 0.2), and the $(dp/dt)_{max}$ is 36.8 MPa/s. As m_l increases to 0.8, the mixture concentration ratio pair (m_g, m_l) is (0.5, 0.8), and the $(dp/dt)_{max}$ is 29.1 MPa/s, which can be mitigated by 19.4%.

As shown in Figure 5c, when the m_g is kept stable, the P_c decreases with an increase in m_l. For example, when m_g = 0.5, the mixture concentration ratio pair (m_g, m_l) is (0.5, 0.2), and the P_c is 10.8 MPa/ (s.m); as m_l increases to 0.8, mixture concentration ratio pair (m_g, m_l) is (0.5, 0.8), and the P_c is 7.8 MPa/ (s.m), which can be mitigated by 18.1%.

3.3.2. Gas Concentration Effect

As shown in Figure 5a, when m_l is kept stable, the P_{max} increases with an increase in m_g. For example, when m_g = 0.2, the mixture concentration ratio pair (m_g, m_l) is (0.2, 0.5), and the P_{max} is 483 kPa; as m_g increases to 0.8, the mixture concentration ratio pair (m_g, m_l) is (0.8, 0.5), and the P_{max} is 537 kPa, which can be increased by 10.4%.

As shown in Figure 5b, when the m_l is unchanged, the $(dp/dt)_{max}$ decreases with an increase in m_g. For example, when m_g = 0.2, the mixture concentration ratio pair (m_g, m_l) is (0.2, 0.5), and the $(dp/dt)_{max}$ is 37.7 MPa/s; when the m_g is 0.8, the mixture concentration ratio pair (m_g, m_l) is (0.8, 0.5), and the $(dp/dt)_{max}$ is 20.1 MPa/s, which can be mitigated by 45.9%.

As shown in Figure 5c, when the m_l is kept stable, the P_c decreases with an increase in m_g. For example, when m_l = 0.5, the mixture concentration ratio pair (m_g, m_l) is (0.2, 0.5), and the P_c is 10.1 MPa/(s·m); as m_g increases to 0.8, the two-phase concentration ratio pair (m_g, m_l) is (0.8, 0.5), and the P_c is 5.4 MPa/(s·m), which can be mitigated by 46.7%.

3.3.3. Influential Analysis

As m_l gets larger, or m_g gets larger, P_{max} increases. The combustion severity effect can be induced to be severe, where red is used to represent the hazard ignition region. However, as m_l gets larger, or m_g gets larger, $(dp/dt)_{max}$ and Pc decrease, mainly due to the ignition time being delayed. A smaller value of $(dp/dt)_{max}$ and P_c usually means the combustion turbulence kinetic energy can be mitigated, where blue is used to represent the energy release rate in a smaller region.

4. Influence of Additive Modified Electrolytes

4.1. Mixture with the Preparation of Additives

4.1.1. Additives' Properties

FEC and VC are the most frequently used electrolyte additives to enhance the lifetime of anode materials in LIBs [20–22]. The properties are listed in Table 4. VC is a new organic film-forming additive and overcharge-protection additive for LIBs that has good high- and low-temperature performance and anti-expansion gas work. The decomposition reaction of FEC reportedly produces F^-. When it reacts with LiPF6 in solvents, it forms LiF, which exhibits high resistance to decomposition. By incorporating LiF insulation, a uniform, compact, low-impedance, and highly elastic SEI film can be formed to effectively suppress the growth of lithium dendrites. Consequently, the addition of FEC improves the flash point and thermal stability of the electrolyte while reducing its volatility, thereby enhancing its flame-retardant performance [23].

Table 4. FEC and VC additives' properties.

Chemical Name	FEC	VC
Molecular formula	$C_3H_3FO_3$	$C_3H_2O_3$
Molecular structure		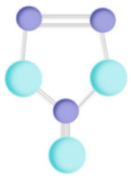
molecular weight	106.05	86.05
Boiling Temperature (°C)	210	165
Flash Temperature (°C)	120	73

4.1.2. Additives Preparation

It is known that the hybrid mixture of non-flammable electrolyte liquid mist and non-flammable gases has the potential to result in severe combustion and a faster burning rate. To prevent ignition and reduce combustion severity, IT should be increased, ignition time should be delayed with combustion turbulence, and kinetic energy should abe mitigated. Therefore, the ignition inhibition strategy using a flame-retardant electrolyte is worth attempting. Table 5 lists battery electrolytes with additive samples.

Table 5. Electrolyte samples with additives.

No.	Electrolyte Lithium Salt	Electrolyte Solvent	Additives
1	1 mol $LiPF_6$	EC:DEC = 1:1 vol%	/
2		EC:DEC = 1:1 vol%	FEC: 5%
3		EC:DEC = 1:1 vol%	FEC: 10%
4		EC:DEC = 1:1 vol%	FEC:10%, VC:1%

4.1.3. Ignition Parameter

According to the experimental procedures explained in Section 2.3.2, the ignition sensitivities parameters and severity parameters of four types of electrolytes in Table 6 can be determined for the LFL, as shown in Table 6 and Figure 6.

Table 6. Ignition parameters for electrolyte samples.

Electrolyte Samples		Sensitivity Parameters			Severity Parameters		
		Concentration (g/m^3)	IT (°C)	Ignition time (ms)	P_{max} (kPa)	$(dP/dt)_{max}$ (MPa/s)	P_C
No.	1	165.5	535	10	550	44.9	12.20
	2	188.5	555	20	585	24.60	6.77
	3	216.5	580	20	600	24.95	6.86
	4	255.5	620	40	623	13.5	3.59

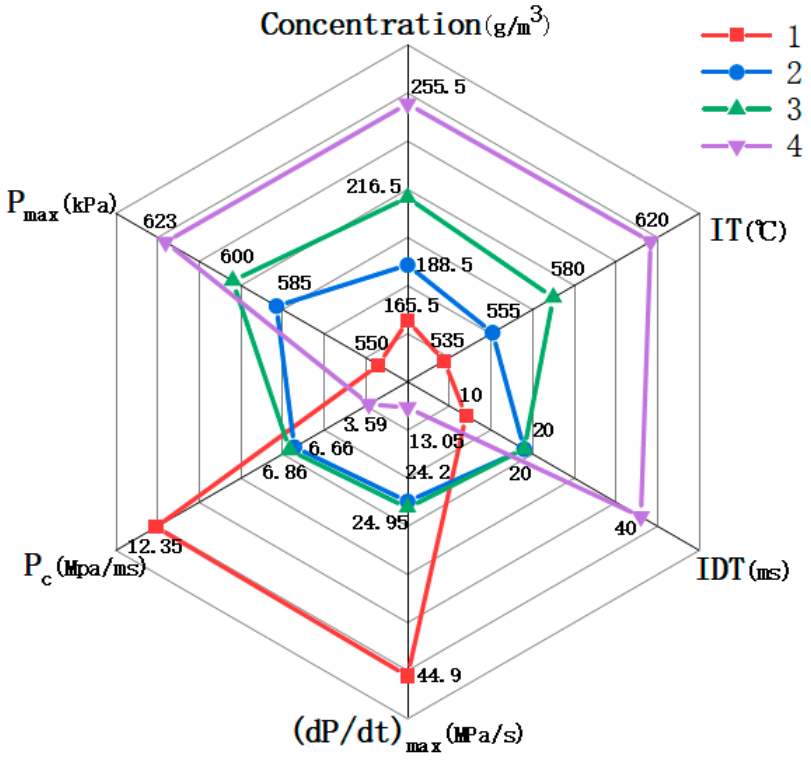

Figure 6. Ignition parameter comparison for electrolyte samples.

IT

As for the ignition temperature, compared to the original electrolyte (No.1), when adding up to 5% FEC (No.2), the IT can only be increased by 4%. When the concentration of FEC is increased to 10% (No.3), IT can be only increased by 8% compared to No.1. Furthermore, No.4 IT can be 620 °C, which improves significantly compared to No.1 by 16%.

Ignition Time

As for the four types of electrolytes, the ignition times are 10, 20, 20, 40 ms, respectively. It can be inferred that adding FEC can defer the ignition time by 2 times. However, the ignition time remains stable as the FEC concentration is increased. However, by adding 1% of VC, the ignition time can be enlarged by 2 times compared to electrolytes No.2 and No.3.

Concentration

Compared to the original electrolyte of No.1, when 5% FEC (No.2) is added, the MEC can be only increased by 12%. When concentration of FEC increased to 10% of No.3, IT can be increased by 30% compared to No.1. Furthermore, the IT for the electrolyte of No.4 can be 255.5 g/m^3, which is a significant improvement by 55% compared to No.1.

Maximum Pressure

The LFL P_{max} values for the four types of electrolytes are 550, 585, 600, and 623 kPa, respectively. Compared to the original electrolyte (No.1), when adding up to 5% FEC (No.2), the P_{max} can be increased by 6%. When the FEC concentration is doubled, the P_{max} can be increased by 9%.

4.1.4. Mixture Fuel with the Preparation of Additives

As per the aforementioned research, when non-flammable gas and liquid are mixed together, the two-phase combination can be ignited. The gas and electrolyte concentrations should be below their LFL, and the gas composition should be identical. As for the battery

venting gas with an LFL of 4.5%, the gas volume concentration in the admixture should be lower than 4.5%. As for the battery liquid electrolyte (No.4) with an LFL of 255.5 g/m^3, the liquid mist mass concentration in the admixture should be lower than 255.5 g/m^3. To determine the ignition conditions for emissions mixtures ignition, the equivalent ratio pairs (m_g, m_l) should be the same as those shown in Table 3, as listed in Table 7.

Table 7. Type No.4 two-phase mixture preparation for the ignition test.

Gas		Electrolyte	
Concentration (vol%)	**m_g**	**Concentration (g/m^3)**	**m_l**
1	11%	15	7%
2	22%	35	14%
3	44%	70	27%
3.5	78%	140	54%
4	90%	210	82%

4.2. Ignition Parameters

4.2.1. Sensitivity Parameters

The IT and ignition time for the No.4 electrolyte mixed with gas can be seen in Figure 7. A non-flammable region also exists, with the mixture concentration ratio pair (m_g, m_l) below (0.3, 0.45).

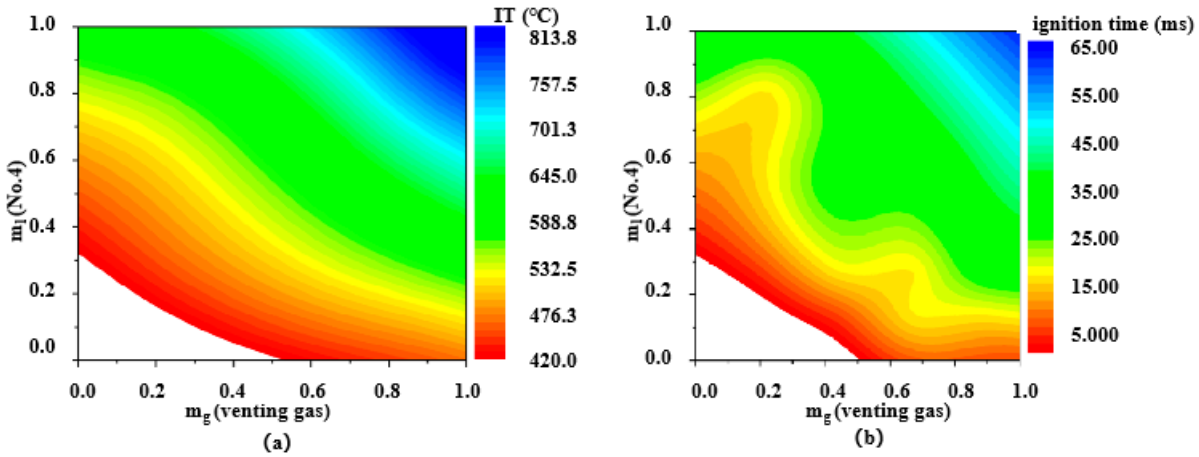

Figure 7. Ignition sensitivity parameters for the gas–electrolyte (No.4) mixture: (**a**) IT, (**b**) ignition time.

Liquid Concentration Effect

As shown in Figure 7a, when m_g is kept stable, the IT gets elevated with m_l increases. For example, when m_g = 0.5, the mixture concentration ratio pair (m_g, m_l) is (0.5, 0.2), and the IT is 458 °C. As the m_l increases to 0.8 from 0.2, the mixture concentration ratio pair (m_g, m_l) is (0.5, 0.8), and the IT is 615 °C, which can be increased by 34.2%.

As shown in Figure 7b, when m_g is unchanged, the ignition time gets delayed while m_l increases. For example, when mg = 0.5, the mixture concentration ratio pair (m_g, m_l) is (0.5, 0.2), and the ignition time is 16 ms. As the m_l increases to 0.8 from 0.2, the mixture concentration ratio pair (m_g, m_l) is (0.5, 0.8), and the ignition time is 33 ms, which can be increased by 1.1 times.

Gas Concentration Effect

When m_l is kept stable, the IT is elevated as m_g increases. For example, when m_l = 0.5, the mixture concentration ratio pair (m_g, m_l) is (0.2, 0.5), and the IT is 472 °C. As the m_g increases to 0.8 from 0.2, the mixture concentration ratio pair (m_g, m_l) is (0.8, 0.5), and the IT is 633 °C, which can be increased by 34.1%.

As shown in Figure 7b, when m_l is kept stable, the ignition time gets delayed as m_g increases. For example, when m_l = 0.5, the mixture concentration ratio pair (m_g, m_l) is (0.2, 0.5), and the ignition time is 17 ms. As m_l increases to 0.8 from 0.2, the mixture concentration ratio pair (m_g, m_l) is (0.8,0.5), and ignition time is 35 ms, which can be increased by 1.05 times.

4.2.2. Severity Parameters

The index parameters of P_{max}, $(dP/dt)_{max}$, and P_c represent the mixture's combustion releases energy. As for the electrolyte of No.4, when mixed with gases, the new type two phases' severity parameters can be seen in Figure 8.

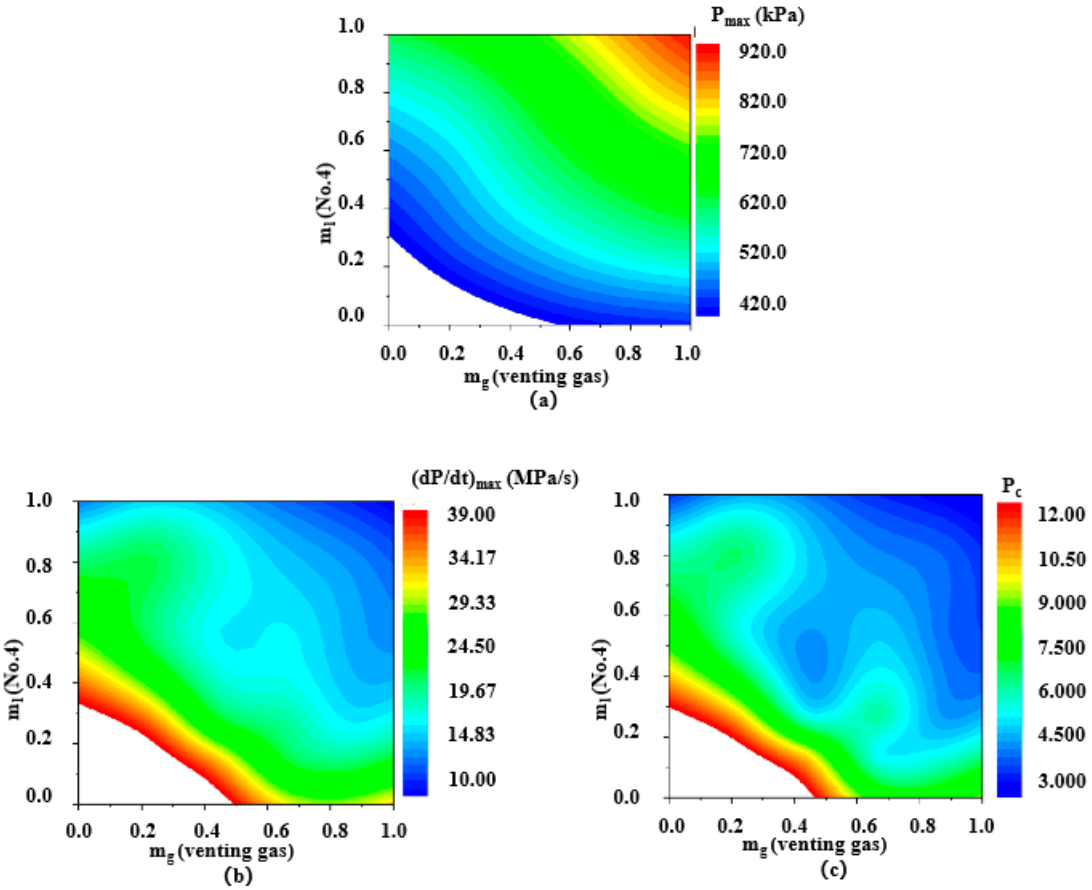

Figure 8. Ignition severity for the gas–electrolyte (No.4) mixture: (**a**) P_{max}, (**b**) $(dP/dt)_{max}$, (**c**) P_c.

Liquid Concentration Effect

As shown in Figure 8a, when m_g is stable, the P_{max} gets increased as m_l increases. For example, when m_g = 0.5, the mixture concentration ratio pair (m_g, m_l) is (0.5, 0.2), and the P_{max} is 482 kPa. As m_l increases to 0.8 from 0.2, the mixture concentration ratio pair (m_g, m_l) is (0.5, 0.8), and P_{max} is 655 kPa, which can be increased by 35.8%.

As shown in Figure 8b, when m_g is stable, the $(dP/dt)_{max}$ gets reduced as m_l increases. For example, when m_g = 0.5, the mixture concentration ratio pair (m_g, m_l) is (0.5, 0.2), and the $(dP/dt)_{max}$ is 25 Mpa/s. When m_l increases to 0.8 from 0.2, the mixture concentration ratio pair (m_g, m_l) is (0.5, 0.8), and the $(dP/dt)_{max}$ is 19 MPa/s, which can be mitigated by 24%.

As shown in Figure 8c, when m_g is kept stable, the P_c decreases as m_l increases. For example, when m_g = 0.5, the mixture concentration ratio pair (m_g, m_l) is (0.5, 0.2), and the P_c is 7.8 MPa/(ms); as m_l increases to 0.8 from 0.2, the mixture concentration ratio pair (m_g, m_l) is (0.5, 0.8), and the P_c is 4.7 MPa/(ms), which can be reduced by 26%.

Gas Concentration Effect

As shown in Figure 8a, when m_l is kept stable, the P_{max} gets elevated as m_g increases. For example, when m_l = 0.5, the mixture concentration ratio pair (m_g, m_l) is (0.2, 0.5), and the P_{max} is 504 kPa. When the m_g increases to 0.8 from 0.2, the two-phase concentration ratio pair is (0.8, 0.5), and P_{max} is 657 kPa, which can be increased by 30.5%.

As shown in Figure 8b, when m_l is stable, the $(dP/dt)_{max}$ decreases as m_g increases. For example, when m_l = 0.5, the mixture concentration ratio pair (m_g, m_l) is (0.2, 0.5), and the P_{max} is 26.2 Mpa/s. As mg increases to 0.8 from 0.2, the mixture concentration ratio pair (m_g, m_l) is (0.8, 0.5), and the P_{max} is 16.3 Mpa/s, which can be reduced by 38.5%.

As shown in Figure 8c, when m_l is kept stable, the P_c gets reduced as m_g increases. For example, when ml = 0.5, the mixture concentration ratio pair (m_g, m_l) is (0.2, 0.5), and the P_c is 7.5 MPa/(ms); as mg increases to 0.8 from 0.2, the two-phase concentration ratio pair is (0.8, 0.5), and the P_c is 4.3 MPa/(ms), which can be reduced by 42%.

4.2.3. Influential Analysis

As m_l or m_g gets larger, P_{max} gets raised, but $(dp/dt)_{max}$ and P_c get reduced. It can be inferred that as P_{max} gets higher, the combustion severity effect can be induced, where red is used to represent the hazard ignition region. However, due to the ignition time effect, smaller values of $(dp/dt)_{max}$ and P_c can be obtained. Smaller values usually mean combustion turbulence kinetic energy is mitigated, where blue is used to represent the hazard reduction region.

4.3. Inhibition Effect Assessment

There is no denying the fact that when adding flame-retardant additives, the ignition sensitivity and severity can change. The flammability inhibition performance between the two types of mixture is compared in this section. The No.1 type mixture is venting gases mixed with original electrolyte (from Table 3), and the No.4 type mixture is venting gases mixed with the No.4 electrolyte (from Table 7).

4.3.1. Sensitivity Parameters

The IT and ignition time comparison between the original one and the electrolyte of No.4 can be seen in Figure 9. Figure 9a clearly shows that the No.4 gas–electrolyte mixture has a higher IT compared to type No.1, especially at a higher m_l and m_g. No.4's maximum IT can be 835 °C, which is 50% larger than No.1's two-phase mixture. This means that the ignition sensitivity is reduced by adding 10% FEC and 1% VC to the electrolyte liquid (1 mol $LiPF_6$ at EC:DEC = 1:1 vol%). However, when the m_g and m_l are in the middle concentration level, the IT is somewhat similar for the two gas–electrolyte mixtures.

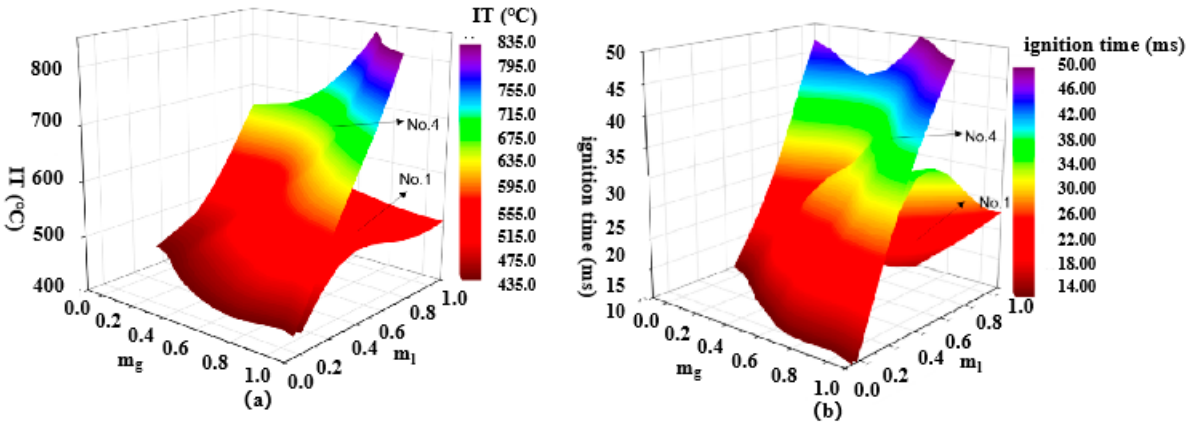

Figure 9. Ignition sensitivity comparison for two types of mixtures: (**a**) IT, (**b**) ignition time.

As for the ignition time, Figure 9b indicates that when m_g and m_l are higher, the ignition time can be higher compared to the type No.1 two-phase mixture. The highest value for the No.4 mixture is 50 ms, which is 40% higher than the No.1 mixture. But when m_l and m_g are at lower or middle concentrations, the ignition time difference between the two gas–liquid mixtures is similar.

Based on the above analysis, it can be concluded that when the concentrations are denser for venting gas and the electrolyte liquid mist, the ignition sensibility can be reduced, which means the flammability can be triggered with some difficulty.

4.3.2. Severity Parameters

The ignition pressure (P_{max}) and $(dp/dt)_{max}$ comparisons between the different two-phase gas–liquid mixtures applied, the original one and the electrolyte of No.4, can be seen in Figure 10. As shown in Figure 10a, the P_{max} indicates that, compared to the type No.1 mixture, when m_g and m_l are larger, the P_{max} gets higher. And the No.4 gas–electrolyte mixture has a much larger value of 820 kPa, which is 32% higher than the No.1 mixture. However, when m_g and m_l are at the low and middle levels, the P_{max} is similar. It can be inferred that as the two-phase concentration gets denser, it has hazardous results for combustion. As shown in Figure 10b, the $(dp/dt)_{max}$ indicates that, compared to the No.1 mixture, when adding 10% FEC and 1% VC to the electrolyte liquid, 1 mol $LiPF_6$ in EC:DEC = 1:1 vol%, the energy release rate can be slightly reduced.

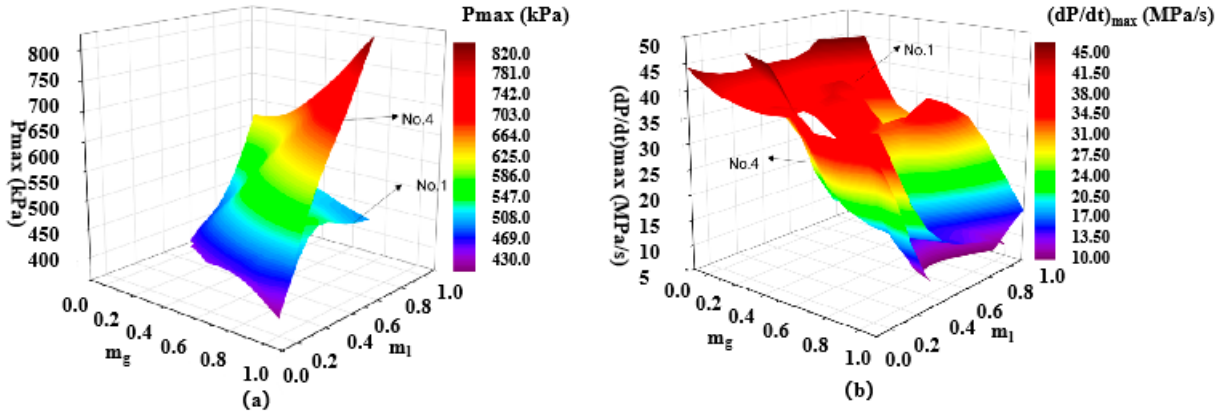

Figure 10. Comparison of two types of mixtures: (**a**) P_{max}, (**b**) $(dp/dt)_{max}$.

5. Conclusions

The flammability characteristics and inhibition effect factors of the LIB emission mixtures' flammability/explosive hazard deserve further research attention. This article has conducted TR experimental research on a 120 Ah $LiFePO_4$ battery in an inert atmosphere. After identifying the components of LIBs' venting emission, a 20 L sphere is adopted to figure out the flammable parameters for the ignition sensitivity and severity for venting gases, liquid mist, their combination mixture, and mixtures with different additives. The main conclusions are as follows:

(1) For 120 Ah $LiFePO_4$, the venting gases components are CH_4, C_2H_6, C_2H_4, C_3H_6, CO, and H_2. And the venting electrolyte is 1 mol $LiPF_6$ in EC:DEC = 1:1 vol%. For gases, including single phase and liquid mist single phase, the sensitivity parameters and severity parameters for LFL have been tested.

(2) For non-flammable venting gases and electrolyte mist, after mixing, the gas–liquid two-phase mixtures can be ignitable. The single-phase ignition boundary condition has a slipping effect. However, there could exist a non-ignition region, where the m_g is below 0.15 and the m_l is below 0.1.

(3) For the gas–liquid mixture, ignition sensitivity parameters from the results in this article show that the gas concentration gets larger, and, as liquid concentration gets

larger, the IT increases. For the ignition severity parameters, as the concentration gets larger and as the liquid concentration gets larger, P_{max} gets raised $(dp/dt)_{max}$ and P_c gets reduced.

(4) For non-flammable electrolytes, 1 mol $LiPF_6$ in EC:DEC = 1:1 vol%, with FEC 10% and VC 1%. When it is mixed with venting gases, this gas–liquid mixture also can be ignited. Compared to the type No.1 two-phase mixtures, the non-ignition region will get wider, where the m_g is below 0.45 and the ml is below 0.3.

(5) The IT maximum value can be 835 °C for type No.4 mixture, which is 50% larger than the No.1 mixture. The highest value for the No.4 gas-electrolyte mixture is 50 ms, which is 40% higher than the type No.1 gas–electrolyte mixture. When adding 10% FEC and 1% VC to the electrolyte liquid (1 mol $LiPF_6$ in EC:DEC = 1:1 vol%), the No.4 type mixture exhibits flame-inhibition effects.

This experimental research proves an innovative methodology to assess battery venting emission safety and non-flammable electrolyte function using a material design principle. Thus, these findings can help to form more suitable preventive and protective measures for commercial EV and BESS thermal safety designs.

Author Contributions: Methodology, Y.L., H.W., L.L., X.F. and M.O.; Software, R.Y.; Writing—original draft, Y.W.; Writing—review & editing, Z.Z. All authors have read and agreed to the published version of the manuscript.

Funding: This research is generously supported by the National Natural Science Foundation of China (Youth Program Grant No. 52207240 & 52207241), Shandong Province Science and Technology Foundation (Youth Program Grant No. ZR2022QE099), and Shandong Province Excellent Youth and Innovation Team Foundation (Grant No. 2023KJ323). The authors gratefully acknowledge the financial support from the Joint Science Foundation of Guangdong Province (Grant No. 21201910260000023).

Data Availability Statement: The original contributions presented in the study are included in the article, further inquiries can be directed to the corresponding author.

Conflicts of Interest: The authors declare no conflict of interest.

References

1. Hu, G.; Huang, P.; Bai, Z.; Wang, Q.; Qi, K. Comprehensively analysis the failure evolution and safety evaluation of automotive lithium ion battery. *eTransportation* **2021**, *10*, 100140. [CrossRef]
2. Wang, H.; Du, Z.; Rui, X.; Wang, S.; Jin, C.; He, L.; Zhang, F.; Wang, Q.; Feng, X. A comparative analysis on thermal runaway behavior of Li (NixCoyMnz) O2 battery with different nickel contents at cell and module level. *J. Hazard. Mater.* **2020**, *393*, 122361. [CrossRef] [PubMed]
3. Lisbona, D.; Snee, T. A review of hazards associated with primary lithium and lithium-ion batteries. *Process Saf. Environ. Prot.* **2011**, *89*, 434–442. [CrossRef]
4. Ouyang, D.; Weng, J.; Chen, M.; Wang, J. What a role does the safety vent play in the safety of 18650-size lithium-ion batteries? *Process Saf. Environ. Prot.* **2022**, *159*, 433–441. [CrossRef]
5. Tran, M.-K.; Mevawalla, A.; Aziz, A.; Panchal, S.; Xie, Y.; Fowler, M. A Review of Lithium-Ion Battery Thermal Runaway Modeling and Diagnosis. Approaches. *Processes* **2022**, *10*, 1192. [CrossRef]
6. Pastor, J.V.; García, A.; Monsalve-Serrano, J.; Golke, D. Analysis of the aging effects on the thermal runaway characteristics of Lithium-Ion cells through stepwise reactions. *Appl. Therm. Eng.* **2023**, *230*, 120685. [CrossRef]
7. Wei, G.; Huang, R.; Zhang, G.; Jiang, B.; Zhu, J.; Guo, Y.; Han, G.; Wei, X.; Dai, H. A comprehensive insight into the thermal runaway issues in the view of lithium-ion battery intrinsic safety performance and venting gas explosion hazards. *Appl. Energy* **2023**, *349*, 121651. [CrossRef]
8. Wei, Z.; Gang, L.; Haoran, Z.; Xiupeng, Z.; Marquez, J.A.D.; Qingsheng, W. Experimental study of explosion parameters of hybrid mixture caused by thermal runaway of lithium-ion battery. *Process Saf. Environ. Prot.* **2023**, *178*, 872–880.
9. Peng, Y.; Yang, L.; Ju, X.; Liao, B.; Ye, K.; Li, L.; Cao, B.; Ni, Y. A comprehensive investigation on the thermal and toxic hazards of large format lithium-ion batteries with $LiFePO_4$ cathode. *J. Hazard. Mater.* **2020**, *381*, 120916. [CrossRef]
10. Wang, Y.; Wang, H.; Zhang, Y.; Cheng, L.; Wu, Y.; Feng, X.; Lu, L.; Ouyang, M. Thermal oxidation characteristics for smoke particles from an abused prismatic Li $(Ni_{0.6}Co_{0.2}Mn_{0.2})O_2$ battery. *J. Energy Storage* **2021**, *39*, 102639. [CrossRef]
11. Wang, H.; Zhang, Y.; Li, C.; Li, W.; Ouyang, M. Venting process of lithium-ion power battery during thermal runaway under medium state of charge. *Energy Storage Sci. Technol.* **2019**, *8*, 1076–1079.

12. Zhang, Y.; Peng, W.; Liu, X.; Jiusheng, R.; Zang, X.; Qi, X.; Jinhua, L. Experimental study on suppression of thermal runaway in lithium-ion battery by mixed particle size water mist. *Process Saf. Environ. Prot.* **2023**, *179*, 189–198. [CrossRef]
13. Xu, J.; Zhang, L.; Liu, Y.; Duan, Q.; Jin, K.; Wang, Q. Electrochemical performance and thermal stability of 18650 lithium-ion battery with water mist after high-temperature impact. *Process. Saf. Environ. Prot.* **2022**, *166*, 589–599. [CrossRef]
14. Pushparaj, R.I.; Kumar, A.R.; Xu, G. Enhancing safety in lithium-ion batteries with additive-based liquid electrolytes: A critical review. *J. Energy Storage* **2023**, *72*, 108493. [CrossRef]
15. Dagger, T.; Grützke, M.; Reichert, M.; Haetge, J.; Nowak, S.; Winter, M.; Schappacher, F.M. Investigation of lithium ion battery electrolytes containing flame retardants in combination with the film forming electrolyte additives vinylene carbonate, vinyl ethylene carbonate and fluoroethylene carbonate. *J. Power Sources* **2017**, *372*, 276–285. [CrossRef]
16. Hu, J.; Jin, Z.; Zhong, H.; Zhan, H.; Zhou, Y.; Li, Z. A new phosphonamidate as flame retardant additive in electrolytes for lithium ion batteries. *J. Power Sources* **2012**, *197*, 297–300. [CrossRef]
17. Sadeghi, B.A.; Wölke, C.; Pfeiffer, F.; Baghernejad, M.; Winter, M.; Cekic-Laskovic, I. Synergistic role of functional electrolyte additives containing phospholane-based derivative to address interphasial chemistry and phenomena in NMC811||Si-graphite cells. *J. Power Sources* **2023**, *557*, 232570. [CrossRef]
18. Cao, C.; Zhong, Y.; Shao, Z. Electrolyte Engineering for Safer Lithium-Ion Batteries: A Review. *Chin. J. Chem.* **2023**, *41*, 1119–1141. [CrossRef]
19. *EN 14034-1-4*; Determination of Explosion Characteristic of Dust Clouds—Determination of the Limiting Oxygen Concentration LOC of Dust Clouds. European Committee for Standardization (CEN): Brussels, Belgium, 2004.
20. Jaumann, T.; Balach, J.; Langklotz, U.; Sauchuk, V.; Fritsch, M.; Michaelis, A.; Teltevskij, V.; Mikhailova, D.; Oswald, S.; Klose, M.; et al. Lifetime vs. rate capability: Understanding the role of FEC and VC in high-energy Li-ion batteries with nano-silicon anodes. *Energy Storage Mater.* **2017**, *6*, 26–35. [CrossRef]
21. Hou, T.; Yang, G.; Rajput, N.N.; Self, J.; Park, S.-W.; Nanda, J.; Persson, K. The influence of FEC on the solvation structure and reduction reaction of LiPF6/EC electrolytes and its implication for solid electrolyte interphase formation. *Nano Energy* **2019**, *64*, 103881. [CrossRef]
22. Ma, C.; Qiu, Z.; Shan, B.; Song, Y.; Zheng, R.; Feng, W.; Cui, Y.; Xing, W. The optimization of the electrolyte for low temperature LiFePO4-graphite battery. *Mater. Lett.* **2024**, *356*, 135594. [CrossRef]
23. Zou, P.; Wang, C.; He, Y.; Xin, H.L. Making Plasticized Polymer Electrolytes Stable Against Sodium Metal for High-Energy Solid-State Sodium Batteries. *Angew. Chem. Int. Ed.* **2024**, *63*, e202319427. [CrossRef]